Temporal Variations of Land Surface Microwave Emissivities over the Atmospheric Radiation Measurement Program Southern Great Plains Site

BING LIN

Center for Atmospheric Sciences, Hampton University, Hampton, Virginia

PATRICK MINNIS

Atmospheric Sciences Research, National Aeronautics and Space Administration Langley Research Center, Hampton, Virginia

(Manuscript received 20 January 1999, in final form 22 July 1999)

ABSTRACT

Land surface microwave emissivities are important geophysical parameters for atmospheric, hydrological, and biospheric studies. This study estimates land surface microwave emissivity using an atmospheric microwave radiative transfer model and a combination of the Special Sensor Microwave Imager (SSM/I) satellite observations and data from the Atmospheric Radiation Measurement Program southern Great Plains (SGP) site during October of 1995. Emissivities are retrieved for both clear and cloudy conditions. Emissivity standard deviations of ~0.035 were found at the SGP site. Much of the variability is produced by a distinct diurnal cycle. The emissivity variability at each SSM/I overpass time (0630, 1100, 1730, and 1000 local time) is about half that for all four times combined. Early morning emissivities are ~0.06 less than those at other times, and the polarization differences at the four times are similar. This behavior is likely the result of dew and surface rewetting effects. Ground observations of dewpoint and temperature difference between air and skin support this theory. The surface emissivities have a significant negative correlation with soil moisture, which can explain about 60%–80% of the emissivity variance when pentad running means are used. Strong correlations among all seven SSM/I channels indicate that the emissivities need to be determined directly for only two or three channels.

1. Introduction

Satellite microwave observations of surface and atmospheric properties have been available over oceans for decades. Near–sea surface wind speed, column water vapor (CWV), cloud liquid water path (LWP), cloud water temperature, and precipitation amount have been studied extensively using the Special Sensor Microwave Imager (SSM/I) data based on either physical or empirical microwave retrieval models (e.g., Goodberlet et al. 1990; Lin and Rossow 1997; Lin et al. 1998b). Quantitative estimation of the surface and atmospheric properties over land regions, however, is limited because of large variations in land surface microwave emissivity. This quantity depends on many other parameters, including frequency, surface roughness and structure, soil type, vegetation, and moisture. The relationships between emissivity and these other variables are not well established in the context of satellite remote sensing. During the past 30 yr, ground and aircraft experimental data and theoretical models have been used to examine the microwave remote sensing of soil moisture (SM) for bare or vegetated soils, snow amount, and the ice depth in freshwater lakes (Ulaby et al. 1986). Efforts to relate these limited studies to the problems of inferring surface emissivity from satellite microwave data are minimal. To begin to address that need, this study uses a combination of ground and satellite data to examine the relationships between surface emissivity and a variety of parameters measured over a partially vegetated land area. Better estimation of microwave surface emissivity would enable the determination of more parameters such as cloud LWP and SM from satellite-observed microwave radiances.

Soil moisture and vegetation coverage are important hydrological variables of the earth's climate. They represent the response of the land surface to atmospheric freshwater flux, solar radiation, temperature, and other atmospheric forcing (Lakshmi et al. 1997). Along with other surface parameters, they affect the depth of the planetary boundary layer, mesoscale circulation, and regional energy and hydrological balance (Rind 1982; Mahfouf et al. 1987). Ground experiments and theoretical studies have revealed strong connections between the microwave land surface emissivities and variations in SM and crop canopy (Ulaby et al. 1986). Using a simulation, Lakshmi et al.

Corresponding author address: Bing Lin, MS 420, NASA Langley Research Center, Hampton, VA 23681-2199.
E-mail: bing@front.larc.nasa.gov

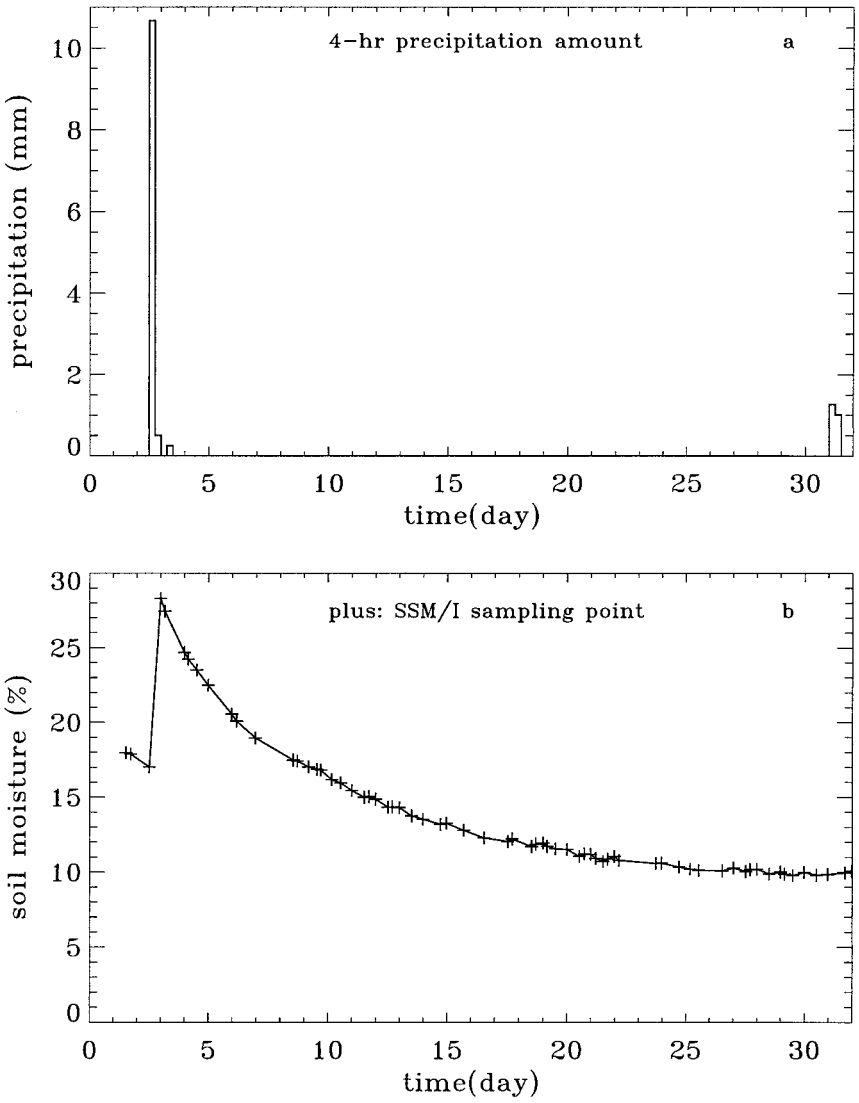

FIG. 1. Ground measurements of (a) 4-h precipitation amounts and (b) soil moisture values at 2.5 cm below the surface. The plus sign in (b) indicates an SSM/I sampling point. Note that UTC is used in the *x* axis in this and subsequent figures.

(1997) showed that satellite microwave data are useful in a regional-scale, land surface hydrological model of SM. Satellite retrievals of surface properties typically use simplified estimates or indices of surface emissivities with no correction for atmospheric attenuation of the microwave radiances. For example, the polarization differences of microwave brightness temperatures observed by satellite microwave radiometers have been used to evaluate surface soil or vegetation properties (e.g., Choudhury 1988; Tucker 1989; Hall et al. 1995). Because the atmospheric components (i.e., CWV, LWP, etc.) affect the brightness temperatures observed from space, these indices do not depend totally on land surface emissivity (Justice et al. 1989; Tucker 1992; Kerr and Njoku 1993; Jackson, 1997).

Jones and Vonder Haar (1997) and Prigent et al. (1997) estimated land surface emissivities for clear scenes using combined satellite microwave, infrared, and visible measurements with physically based atmospheric microwave radiative transfer models. The infrared and visible data are used mainly for cloud screening, land surface skin temperature estimation, and water vapor retrieval. The radiative transfer model is used to minimize the errors caused by atmospheric attenuation of the upwelling radiances. These studies found that the average retrieval errors and day-to-day variations of the emissivities are about 0.01 for certain time periods.

Although the average surface emissivity variations on a large scale may be not substantial if land and vegetation types do not change dramatically, variances at the regional scale could be large. Field experiments found that surface emission for frequencies between 1 and 10 GHz is strongly affected by the diurnal variations of SM and temperature

TABLE 1. Mean and standard deviation of surface emittance. The 19*P*, 37*P*, and 85*P* values are the polarization differences of the land surface emittance at 19, 37, and 85 GHz, respectively.

19v	19h	22v	37v	37h
0.9580 ± 0.0327	0.9322 ± 0.0344	0.9524 ± 0.0310	0.9466 ± 0.0324	0.9242 ± 0.0335
85v	85h	19P	37P	85P
0.9449 ± 0.0323	0.9257 ± 0.0331	0.0258 ± 0.0074	0.0224 ± 0.0066	0.0191 ± 0.0067

(Raju et al. 1995). Theoretically, plant water content, which may also have strong diurnal variations, is another factor affecting the microwave emission (Le Vine and Karam 1996). Airborne microwave remote sensing and ground radar observations (Ulaby et al. 1986) have shown large variances in emissivities caused by changes in vegetation and SM. Jones and Vonder Haar (1997) detected small (about 0.01) diurnal variations over areas in southern Texas and western Mississippi using satellite microwave observations but did not analyze the diurnal variability in detail. The unknown diurnal variations of land surface emissivities may have a large effect on the application of satellite microwave remote sensing to the measurement of clouds and surface hydrological parameters.

This study uses combined satellite and ground observations to focus on the temporal (especially diurnal) variability of land surface microwave emissivities and the relationships between the emittance and other geophysical parameters. The satellite microwave data are obtained from SSM/I measurements, and the ground data were taken by Atmospheric Radiation Measurement (ARM) Program instruments at the southern Great Plains (SGP) site. Land surface microwave emissivities can be derived for both clear and cloudy conditions because ARM up-looking surface microwave radiometer data are used. The next section describes the land surface microwave emissivity retrieval scheme and the satellite and ground observational datasets. Section 3 presents the retrieval results and discusses the effects of SM, precipitation, and surface wetness on the emissivities. The concluding remarks are given in section 4.

2. Methodology and datasets

The technique used to retrieve land surface microwave emissivity is based on a plane-parallel atmospheric microwave radiative transfer model (MRTM) and has been used to determine cloud LWP, precipitation, and other parameters over oceans (Lin et al. 1998a,b). The model physically accounts for the absorption by atmospheric gases and cloud liquid water. Inputs to the model include vertical distributions of atmospheric temperature and gas abundance, cloud LWP and height, and land surface skin temperature. The only unknowns for the model are the land surface microwave emissivities. The SSM/I-measured brightness temperatures (Tb_i), where i means the ith channel of SSM/I, correspond to the true top-of-atmosphere (TOA) microwave radiances. The procedure to retrieve the emissivities for all seven SSM/I channels is the same. The retrieval for the ith channel of SSM/I starts with prescribed minimum (0.2) and maximum (1.2) land surface microwave emissivities followed by several steps.

1) The respective minimum and maximum values, $\varepsilon_{\min i}$ and $\varepsilon_{\max i}$, are selected such that the SSM/I-observed Tb_i values are within the range of the model-calculated TOA microwave brightness temperatures.
2) New emissivities $\varepsilon_{\mathrm{new}\_i}$ are computed for the ith SSM/I channel according to the rule of golden section, that is, $\varepsilon_{\mathrm{new}\_i} = 0.618(\varepsilon_{\max i} - \varepsilon_{\min i}) + \varepsilon_{\min i}$, and used to simulate the TOA microwave brightness temperatures again.
3) The results then are compared with Tb_i, and the maximum values are replaced by new emissivities if the simulated temperatures are larger. Otherwise, the minimum values are replaced.
4) Steps 2 and 3 are repeated until $\varepsilon_{\max i}$ minus $\varepsilon_{\min i}$ is less than 0.0001 and the differences between simulated and observed temperatures are within ±0.1 K. The retrieved emissivities ε_i are the golden section values of the final minimum and maximum land emissivities.

This study uses satellite microwave and ground measurements taken 1–31 October 1995 over the ARM SGP site centered at 36.5°N, 97.6°W. The microwave satellite data are from SSM/I on the Defense Meteorological Satellite Program (DMSP) *F-10* and *F-13* satellites. The DMSP *F-10* and *F-13* passed over the SGP site near 1100 and 2200 local time (LT) and near 0630 and 1730 LT, respectively. SSM/I measures radiances at frequencies of 19.35, 22.235, 37.0, and 85.5 GHz (hereinafter referred to as 19, 22, 37, and 85 GHz). Vertical (v) and horizontal (h) polarization measurements are taken at all frequencies, except at 22 GHz for which SSM/I has only a vertically polarized channel. Spatial resolutions of SSM/I observations depend on frequency, varying from ~13 km at 85 GHz to ~60 km at 19 GHz. The ground observational data used in this study were measured by two-channel microwave radiometer (MWR), surface meteorological observation system (SMOS) instruments, energy balance Bowen ratio (EBBR) station, Belfort Instrument Company laser ceilometer (BLC), and solar and infrared radiation observing system (SIROS). These ground observational data (Stokes and Schwartz 1994) are used as the inputs for MRTM or for analysis of the results. Because surface observations provide all of the inputs to MRTM, the land surface

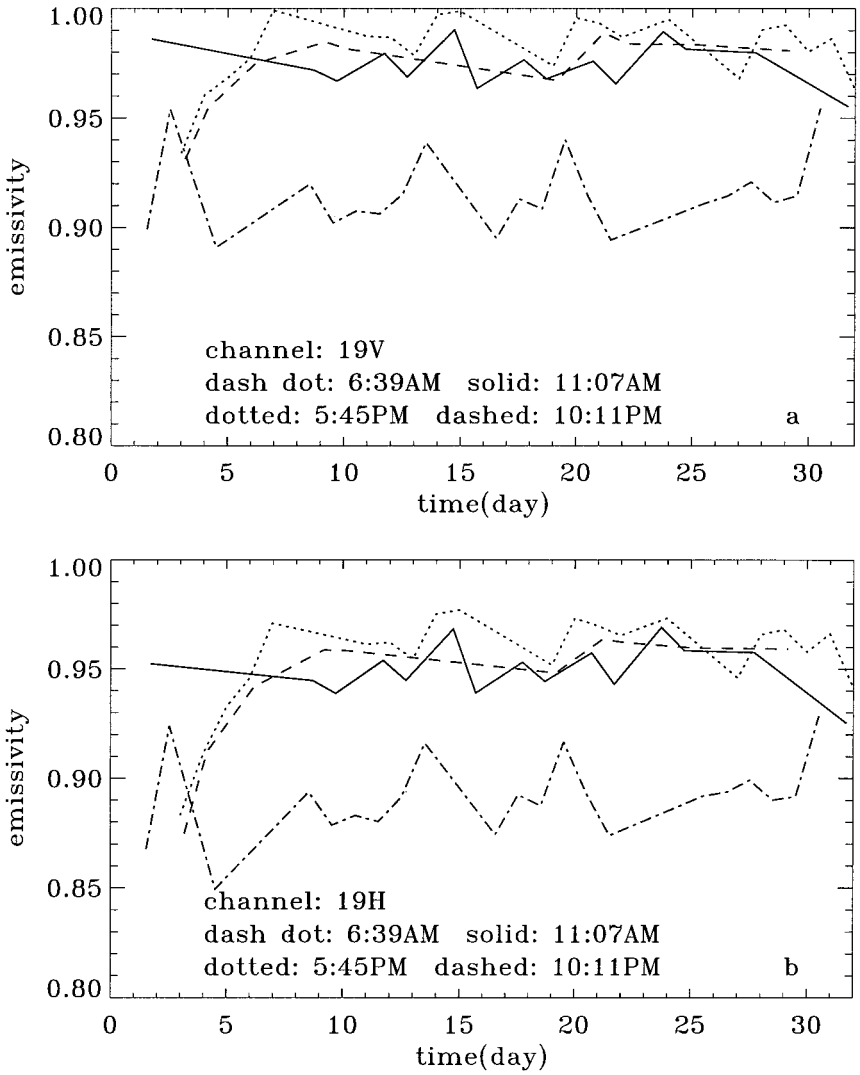

FIG. 2. The emissivities at 19 GHz [(a) vertical and (b) horizontal polarizations, respectively] for four different overpasses. The times listed in the figure are mean local times for the SSM/I overpasses.

microwave emissivities can be derived for both clear and cloudy conditions.

Both cloud LWP and temperature significantly affect microwave radiation (Lin et al. 1998a,b). Therefore, the MWR-observed LWP and BLC cloud height are used in the simulations. The vertical distributions of atmospheric temperature and gas abundance are based on climatological profiles (McClatchey et al. 1972) interpolated to conform to the SMOS surface air temperatures and the MWR CWV data. The estimated emissivities are sensitive to surface skin temperature T_s (about 0.006 K^{-1}; see Prigent et al. 1997). Here, the T_s values used in MRTM are derived from SIROS upwelling and downwelling broadband longwave fluxes and are obtained from the Clouds and the Earth's Radiant Energy System Project (CERES)/ARM/Global Energy and Water Cycle Experiment (GEWEX) Experiment (CAGEX; Charlock and Alberta 1996). The retrieval of T_s assumes a constant surface broadband longwave emissivity of 0.981. This value is essentially the same as the one used by Jones and Vonder Haar (1997). The mean SM data averaged from the EBBR-5 measurements at 2.5 cm below the soil surface are compared to ε_i. Precipitation and near-surface wind speeds were taken from the SMOS data. Because the surface measurements were taken at different rates, from 20 s (MWR) to 0.5 h (e.g., SMOS), all of the parameters were averaged into 0.5-h segments. At the time of writing, the ARM data and their detailed descriptions could be obtained through the Internet (http://www.archive.arm.gov/cgi-bin/arm-archive).

The SSM/I and surface datasets were collocated into 0.5° lat × 0.5° long grid boxes to within ±15 min. The SSM/I sampling rates and the missing satellite and surface observations together limited the study to a total

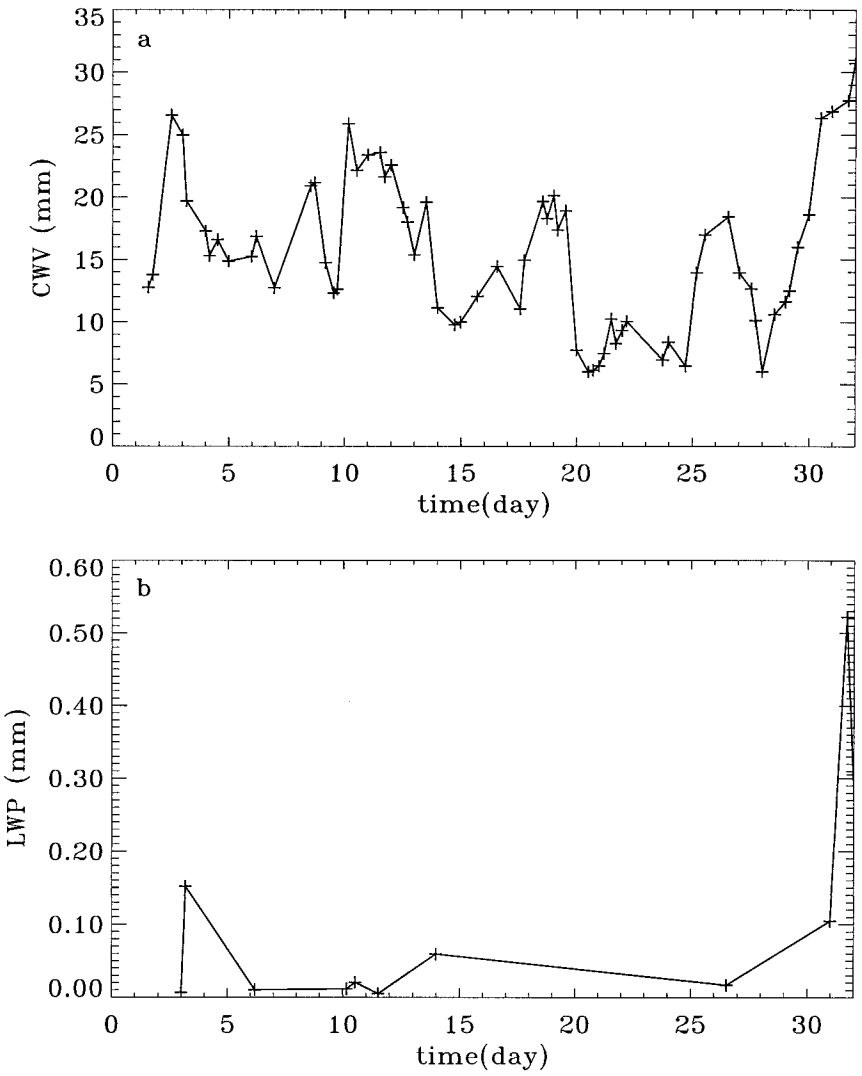

FIG. 3. The ARM MWR measurements of (a) CWV and (b) LWP for the collocated SSM/I overpasses.

of 69 cases. For each case, the reported emissivities are the averaged results for all matched pixels. Only 13 cases are under cloudy conditions.

Figure 1 shows the ARM measurements of the 4-h accumulated precipitation and SM levels within the month. The SSM/I sampling times are indicated by the plus (+) signs in Fig. 1b. Precipitation occurred at the beginning (2–3 October) and end of the month (Fig. 1a). Soil moisture increased sharply after the first rains and then decreased exponentially (Fig. 1b). At the end of the month, the light precipitation had little effect on SM at 2.5 cm below the surface, probably because of rapid evaporation and the generally desiccated surface skin layer. The dynamic range of SM for this period is determined by the major rainfall event. These SM data provide an excellent example of the transition from a wet to a dry surface. The surface types around the ARM site are mainly grasslands and winter wheat fields (at least 50%). During most of October, many of the winter wheat fields were bare soil because of recent plowing and planting. Soil moisture in such bare areas can have a direct influence on the microwave emission and, hence, the SSM/I measurements. Although land surface microwave emissivity varies with SM, the emission depths are only about 1/10–1/4 of the microwave wavelength. For the SSM/I 19-GHz channels, this means the dominant layer is on the order of 0.4 cm (Jackson 1997). It is expected that the near-surface SM is generally uniform for grasslands and may vary with depth under desiccated condition in winter wheat fields. The EBBR measurements more or less represent the moisture of the top soil layer (about 0–5 cm).

3. Results and discussion

The derived values of ε_i and their relationships with the observed meteorological and hydrological parame-

TABLE 2. Mean and standard deviation of surface emittance for the four overpasses. The local times are used.

	0630	1100	1730	2200
19v	0.9155 ± 0.0174	0.9746 ± 0.0097	0.9815 ± 0.0157	0.9731 ± 0.0169
19h	0.8912 ± 0.0183	0.9500 ± 0.0113	0.9549 ± 0.0224	0.9439 ± 0.0272
22v	0.9123 ± 0.0168	0.9691 ± 0.0097	0.9723 ± 0.0158	0.9698 ± 0.0162
37v	0.9039 ± 0.0161	0.9664 ± 0.0108	0.9688 ± 0.0142	0.9602 ± 0.0155
37h	0.8830 ± 0.0168	0.9459 ± 0.0123	0.9453 ± 0.0189	0.9337 ± 0.0251
85v	0.9065 ± 0.0148	0.9609 ± 0.0292	0.9640 ± 0.0165	0.9611 ± 0.0137
85h	0.8894 ± 0.0167	0.9430 ± 0.0303	0.9450 ± 0.0179	0.9357 ± 0.0244
19P	0.0243 ± 0.0049	0.0245 ± 0.0037	0.0266 ± 0.0084	0.0292 ± 0.0112
37P	0.0210 ± 0.0043	0.0205 ± 0.0033	0.0235 ± 0.0066	0.0265 ± 0.0105
85P	0.0171 ± 0.0041	0.0178 ± 0.0034	0.0190 ± 0.0049	0.0254 ± 0.0119

ters are examined here with a focus on the temporal (especially diurnal) variations of surface emissivities. Polarization differences Δp (i.e., the differences between vertically and horizontally polarized emissivities: $\varepsilon_v - \varepsilon_h$) also are discussed.

a. Diurnal variations of emissivity

Analysis of the SSM/I data revealed precipitating clouds in 2 of the 69 cases. These results were confirmed by ground observations. The MWR-estimated LWP values for these two cases, observed during the first week of the month, are extremely large (about 11.5 and 3.5 kg m^{-2}) and may be out of the instrument's linear response regime. Because the vertical profiles of the precipitation are unknown, no emissivities were retrieved for these two rainfall cases. Table 1 lists the means and standard deviations of all emissivities of SSM/I channels. This table shows that ε_i is strongly wavelength dependent and variable with standard deviations exceeding 0.03. The emissivities with v polarization are generally greater than those with h polarization, although the differences are not very big, ranging from 0.020 to 0.026. Jones and Vonder Haar (1997) observed the same general tendency. The large ε_i variations shown in Table 1 would produce large errors in cloud LWP, CWV, and other atmospheric properties derived from SSM/I data over land regions (cf. Prigent et al. 1997). Mean values of ε_i are slightly less (differences <0.005) than those of Jones and Vonder Haar (1997) and may reflect wetter conditions or differences in vegetation.

Emissivities for cloudy skies are slightly lower than those for clear conditions. Their differences vary from about -0.009 for v polarization to about -0.014 for h polarization. The standard deviations for both clear and cloudy conditions are about the same as those for the original data listed in Table 1. The polarization differences for cloudy skies, on the other hand, are about 0.004 larger than those for clear cases. Because cloudy conditions may reduce evaporation from the surface and are associated temporally with precipitation, ε_i should be lower, and the polarization difference could be higher, because ε_h is more sensitive to moisture than ε_v is. Because there were fewer cloudy cases than clear cases, and the mean differences are within the variances of the datasets (Table 1), the differences in ε_i and Δp between clear and cloudy skies are not statistically significant. Analysis of a larger dataset may produce a more conclusive result.

To understand the large variability found here, the data were separated into four different times corresponding to each satellite overpass. Figure 2 shows the time series of ε_{19v} and ε_{19h} at the four local times (note that the basic features of ε_i for other SSM/I channels are the same as those shown here). The atmospheric water vapor and cloud liquid water amounts are plotted in Fig. 3. The atmospheric moisture generally decreases after the major precipitation, with about 10 mm oscillation (Fig. 3a). The CWV oscillation may be related to large-scale weather variations, as indicated in LWP data (Fig. 3b). As expected, there are no significant correlations among CWV, LWP, and the emissivity values. To obtain ground-level brightness temperatures (or emissivities) using SSM/I observed values, the atmospheric corrections vary from ~0.1 to 3 K depending on the atmospheric conditions, wavelength, and polarization. It could introduce large errors (about 0.01) in estimated emittance in comparison with the standard deviations of ε_i (cf. Table 2 for means and standard deviations) if a constant 3-K correction is used (Jackson 1997). Emissivities from *F-13* at 0640 LT are considerably lower than those for the other three passes. No significant differences in ε_i are evident between the near-noon, evening, and early-night passes. The differences in ε_i between the pass at 0640 LT and other passes are about 0.06, a value much larger than the standard deviations within each time segment. This separation between the two groups of data is clearly evident in Fig. 2. The standard deviations in ε_i for each local time are ~0.015 in comparison with 0.03 for the original data. Thus, most of the original variability is due to the diurnal difference demonstrated in Fig. 2. Exceptionally large variations in ε_i occur at 85 GHz near noon when the standard deviations (about 0.03) are only slightly less than the original values. The estimated emissivities at 85 GHz are affected strongly by precipitation. If the data near rainfall events are eliminated, the standard deviations drop to less than 0.01.

The polarization differences for the four local times

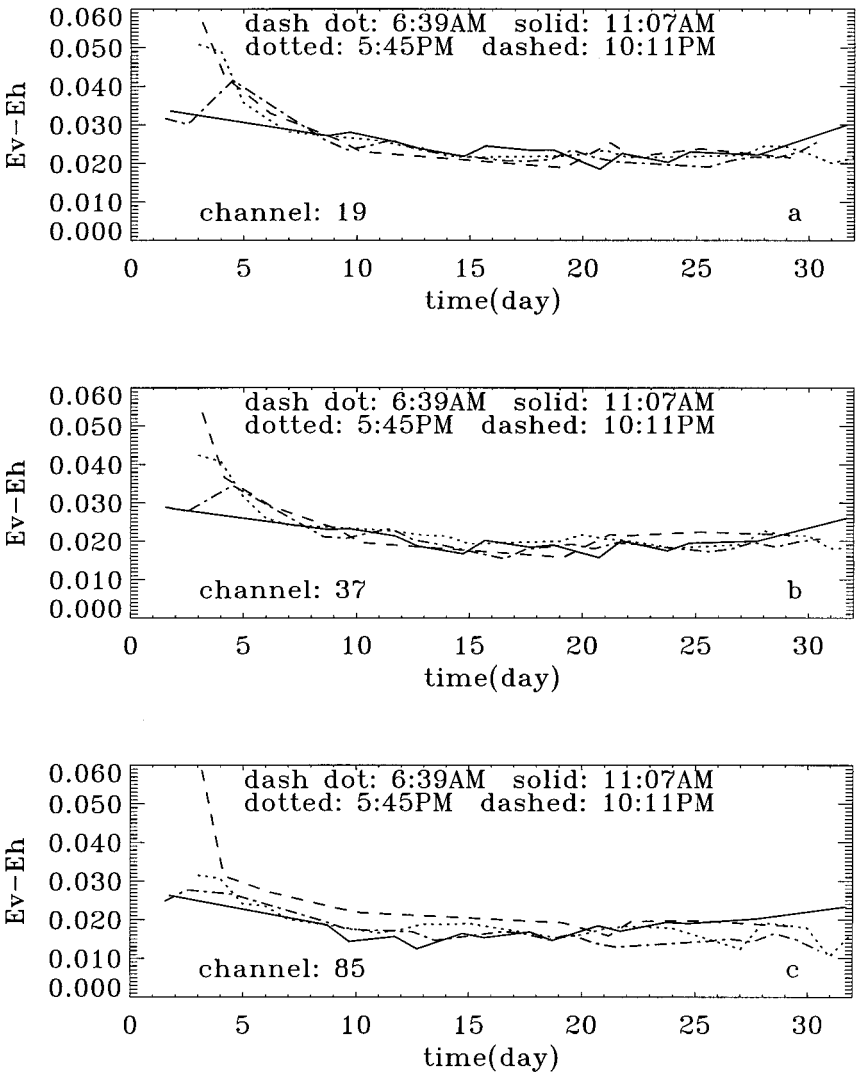

FIG. 4. Same as Fig. 2 but for polarization differences at all SSM/I frequencies [(a), (b), and (c) correspond to different channels, as labeled].

are generally the same, and the higher the frequency is, the lower the differences are (Fig. 4). Large differences, especially for the nighttime overpasses, occurred shortly after rainfall (cf. Fig. 1), suggesting the influence of increased surface water. The means and standard deviations of Δp (Table 2) are similar to those of the original data (cf. Table 1). If precipitation is avoided, the standard deviations for all four times are very small (<0.004) as seen in the smooth middle sections of the curves in Fig. 4. The small polarization differences among the four times for all frequencies are in contrast to the large diurnal variations in ε_i, implying that the physical factors producing large decreases in ε_i at 0640 LT may have similar effects on both v and h polarizations.

Figures 2 and 4 obviously exhibit the effects of precipitation on ε_i derived from 3 and 31 October data. During 3 October, the *F-13* and *F-10* satellites passed over the SGP site at 1745 LT and 2211 LT, respectively, only a few hours after the major rainfall of 2 October (cf. Fig. 1). The values of ε_i were significantly depressed for both cases (cf. the beginning of dotted and dashed curves in Fig. 2). Similarly, the minor rainfall early during 31 October is reflected in a large decrease in ε_i for the overpass at 1107 LT (cf. the end of the solid curves in Fig. 2). The emissivities for the precipitation cases at all seven SSM/I channels are about 0.03–0.08 smaller than their background values. The decreases in ε_i after precipitation would be even bigger if there were no rain water interception by vegetation (Wigneron et al. 1996).

The big decreases in ε_i result from soaking of the surface by rain. Liquid water surfaces generally have much lower emissivities than do dry land surfaces. An

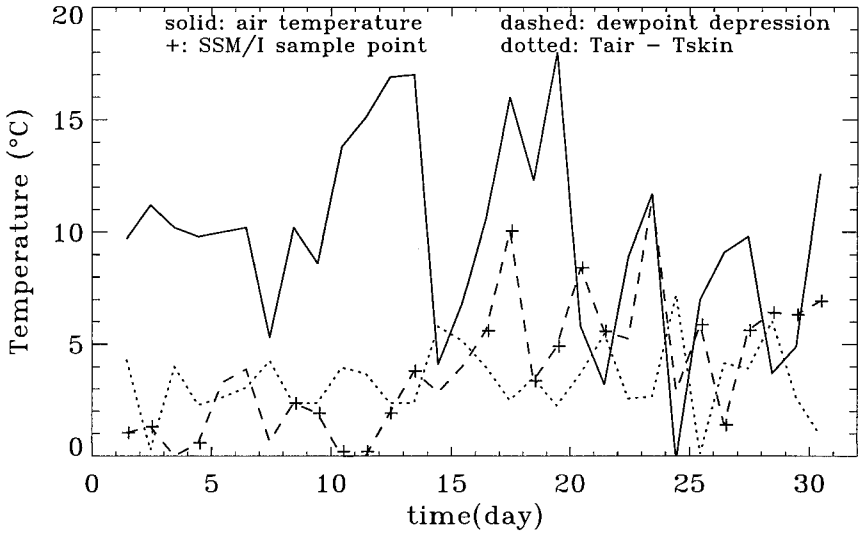

FIG. 5. Ground-measured 3-h mean values from 0300 to 0600 LT of surface air temperature (solid), dewpoint depression (dashed), and the temperature differences between surface air and skin (dotted). Plus sign indicates an SSM/I sampling point.

extreme case is the ocean surface, for which the emissivities are about 0.5. Many studies have found low values of ε_i because of rainfall (e.g., Raju et al. 1995). For example, Jones and Vonder Haar (1997) found that rain events frequently modify the emissivity over the central Great Plains and cause noticeably lower values within a 1-week period. Comparing rainfall amounts and microwave surface emissivities, Prigent et al. (1997) have shown that the extension of the Zambezi swamps agrees well with the low microwave emissivities caused by precipitation. In contrast to changes in ε_i, the polarization differences (Fig. 4) are greater after a rainfall, a phenomenon consistent with theory and observations, as discussed by Jones and Vonder Haar (1997) and Prigent et al. (1997). Figures 2 and 4 show that ε_i recovered to its normal values approximately 2–3 days after the precipitation. This time period is close to or slightly shorter than the time elapsed between the precipitation and the return of SM to dry conditions (cf. Fig. 1).

The low emissivities at 0640 LT (Fig. 2 and Table 2) are likely the result of other effects. The most important factors depressing ε_i may be dew and surface rewetting. Dew water on land surfaces could be considered as water droplets and/or small facets. In the former case, the droplets are large enough (in comparison with SSM/I wavelengths) to produce significant scattering and absorption. In the latter case, the water layers absorb some of the microwave radiation emitted from the soil and vegetation and reflect downwelling microwave radiation back into the atmosphere. Both scattering and absorption decrease the apparent land surface emissivity. Ground experiments (Ulaby et al. 1986) found that microwave backscattering considerably increased (by about 3 dB) when leaves held water droplets and gradually dropped to normal levels after the water on the leaf surfaces evaporated. The small differences in Δp among the four local times for all frequencies and the slightly diminished values at 0640 LT (cf. Fig. 4 and Table 2) also seem to support this hypothesized dew effect. Although the equal absorption of v- and h-polarized radiation by water reduces Δp, the scattering and reflection processes increase Δp. The net effect of dew on Δp could be small or even negative. Dew may affect ε_i in a manner similar to that of rainfall but may have much less effect on the polarization differences. The exact reasons for the differences are unknown, but they may be due to large amounts of rainwater at the soil surface, which would not only reduce ε_i but also increase Δp.

Because of the surface skin cooling at night, land surfaces around the ARM SGP site may have undergone rewetting. The surface and soil can obtain moisture from both condensation and infiltration during the night. Rewetting of the soil surface has effects on ε_i similar to those of rainwater. Thus, the moisturized surface layers would cause low emissivity values.

Over the ARM SGP site, dew and rewetting were common during the month because of large diurnal temperature variations (about 10 K). Figure 5 shows the 0300–0600 LT mean values of surface air temperature, dewpoint depression, and the difference between air and skin temperatures for the month. The SSM/I 0640 LT sampling points also are indicated in the figure. The day-to-day changes in the early-morning air temperature ranged from about 5° to 15°C, which, along with other parameters such as CWV (cf. Fig. 3), led to variations in relative humidity. All dewpoint depression values were less than 12 K. Most did not exceed 6 K. Skin temperatures were about 0.5–5 K lower than air temperature and similar to or less than the dewpoint (i.e.,

the temperature differences between air and skin were greater than dewpoint depressions). These results suggest that dew formed during most mornings, especially during those when SSM/I passed over the site.

Two SSM/I-observed cases (17 and 20 October) had very large (about 10 and 8 K) dewpoint depressions. Using both ground and satellite shortwave (and visible) observations, Minnis et al. (1997) found that the surface broadband albedo values were significantly affected by dew for the same period of this study over the SGP site. The dew effects caused asymmetry in the diurnal variations of the surface albedo and increased the land surface reflectance. They inferred dew formation for 20 October but did not have the data for 17 October. Surface records revealed dewpoint depression values of ~6 K during early morning before the SSM/I overpass on 17 October. Furthermore, ground meteorological observations reported that fog formed during the morning (S. Kato 1998, personal communication). Because the ARM ground microwave measurements reported zero cloud LWP for the morning (Fig. 3), and the absorption of light fog would slightly decrease upwelling microwave radiation, these analyses probably would underestimate ε_i in such cases. Although the diurnal signals were weak, Jones and Vonder Haar (1997) found that dew decreased the emissivities for morning overpasses by about 0.01 over south Texas. Their depressions are smaller than those in Table 2. The discrepancies may be due to averaging differences over different spatial and temporal scales, to differences in surface properties and dew loading, and to the errors in ε_i of this study (see later). If emissivities were averaged only according to morning and afternoon overpasses, the diurnal differences in ε_i would be almost half of the current values in Table 2 and Fig. 2. Furthermore, values of water amount over soil and vegetation surfaces and dew droplet size are more or less localized, depending on temperature, relative humidity, and other land surface properties.

Another reason for diminished early-morning emissivities is the vertical SM profile. During early morning, SM is more uniform with depth, and, at other times, especially during afternoon, the surface skin layer is drier. For SSM/I wavelengths, the skin layer is the major contributor of land surface emission to the satellite-observed radiances. The vegetation moisture content is also higher during morning. Increases in soil and vegetation moisture could decrease the surface emissivities (Ulaby et al. 1986; Calvet et al. 1995a,b; Le Vine and Karam 1996) during the night after the subsurface moisture has been drawn to the upper layers.

Other factors causing the low values of ε_i for early-morning overpasses or big differences (about 0.06; cf. Table 2) between ε_i during early-morning overpasses and during other overpasses are possible errors in estimating skin temperature. For this study, the broadband longwave emissivity ε_{IR} used in retrieving T_S is assumed to be a constant (0.981). Because of stronger absorption of water than that of soil, dew effects would increase the land surface ε_{IR} values, and in dry soil conditions ε_{IR} can be as low as 0.96 (Salisbury and D'Aria 1992). Minnis et al. (1998) have shown that ε_{IR} for a wavelength of 11 μm can vary from 0.965 to 0.995 over the south-central Great Plains depending on the season and surface conditions. Under-/overestimation of ε_{IR} would over-/underestimate the skin temperature, especially in clear sky conditions, leading to negative/positive biases in ε_i. For this study, ε_{IR} errors between dry and wet conditions could be about 0.04, which would produce an ε_i error as large as about 0.01. Also, potential ε_i errors may result from the estimation of skin temperature itself. Although T_S values are generally uniform over the scale of SSM/I footprints, *GOES-8* 4-km pixel data in a 0.5° region show that T_S has a spatial standard deviation of ~0.4°C during the local morning times. For small T_S errors of ~3 K, errors in ε_i could be as large as 0.01. Furthermore, the errors in other ground measurements could exaggerate the ε_i errors from these two effects. If the ε_i errors in estimating T_S are about 0.03, the ε_i gap between A.M. and P.M. SSM/I overpasses would shrink to about 0.015, which is close to the differences reported by Jones and Vonder Haar (1997).

b. Effects of soil moisture on emissivity

Because there are large areas of winter wheat around the ARM site, the estimated ε_i values should be correlated to the ARM SM measurements during October, because those fields are primarily bare soil because of recent plowing and planting. The SM effects on ε_i are clearly evident in Table 2 and have been observed in other studies (e.g., Jackson 1997). The emissivities for all SSM/I channels generally change from low early-morning values to high near-noon values to maximum values during early evening and then decrease slightly to levels similar to the near-noon values. This cycle presumably occurs because of the changes in the amount of water on vegetation surfaces and in SM amounts. The latter factor would be most effective in driving the changes in ε_i from 1100 to 2300 LT because late afternoon is usually the driest time of day.

In comparison with the smooth decrease of SM during the month (Fig. 1), the trends in ε_i values are not very clear (Fig. 2). Large variations at short timescales can hide the trends. Vegetation water content and coverage can also affect microwave radiation (or weaken the signals) from soil surface (Jackson and Schmugge 1991; Calvet et al. 1995a; Wigneron et al. 1996). Because short-lived dew effects may modulate ε_i dramatically, the SSM/I estimated emissivity could be decoupled from SM. Thus, by excluding the data from the overpass at 0640 LT and using a low-pass filter, it should be possible to determine the relationship between SM and ε_i. Figure 6 shows the pentad running means without early morning data. The general trend in Fig. 6 suggests that ε_i increases during the month, which is strongly correlated with SM (cf. Fig. 1).

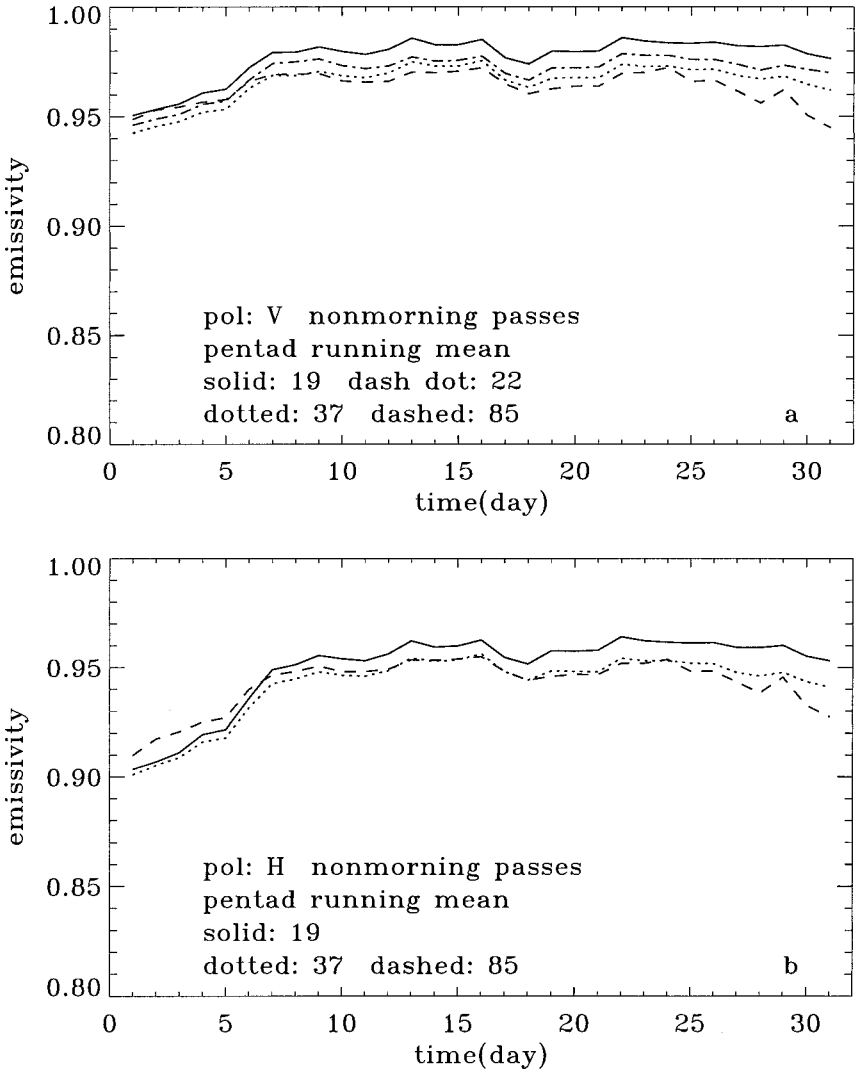

FIG. 6. Pentad running mean values of the microwave emittance for (a) vertical and (b) horizontal polarizations, with early-morning data excluded.

Figure 7 shows the scatterplots and correlation coefficients of the running mean values of ε_i and SM for the 19- and 22-GHz channels without the data from 0640 LT. The emissivities are negatively correlated with SM, with a statistical significance well above the 99% confidence level. In general, the emissivities for h polarization channels (or lower-frequency channels) are more dependent on moisture than those for v polarization channels (or higher-frequency channels). The high values of SM (>20%) correspond to the samples taken shortly after the major rainfall and provide sufficient dynamic range to develop the correlations. The saturated ε_i values are associated with desiccated soil (SM < 12%). In this case, the soil moisture at 2.5 cm below the surface may be decoupled from that of the microwave emission layer (top 0.4 cm of the surface). Depending on the channel, SM can explain about 60%–80% of the spectral emissivity variances. The remaining variance is due to other factors such as vegetation moisture, soil dielectric properties, effective soil temperature, and near-surface wind speed. Even changes in SM profiles can affect land surface microwave emission (Raju et al. 1995), thereby decreasing the correlation between satellite-estimated emissivity and ground-measured SM at a depth of 2.5 cm.

Because higher frequencies generally are more sensitive to shallower surface layers than are lower frequencies (Raju et al. 1995), the soil thickness remotely sensed by the 85-GHz channels is much thinner than those thicknesses sensed by the lower-frequency SSM/I channels. This insensitivity to changes deeper in the soil decreases the coupling between the retrieved 85-GHz emissivities and the ground measurements of SM. The Δp values have even stronger correlation with SM than

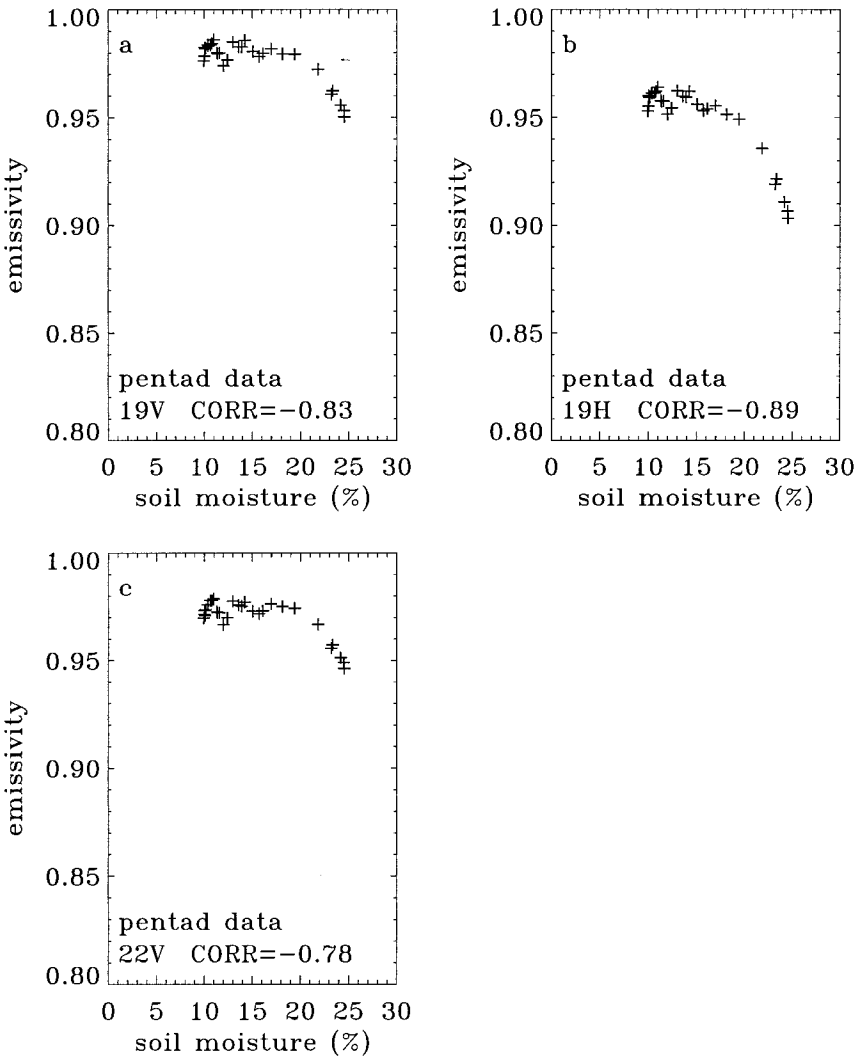

FIG. 7. Scatterplot of the pentad running mean emissivity vs soil moisture values with early-morning data excluded. CORR is correlation coefficient. Here (a), (b), and (c) correspond to different channels and polarizations, as labeled.

those of ε_i. The SM can explain about 80%–90% of the variance in Δp in these cases. The relationship probably is even stronger when extreme dry conditions (SM $<$ 12%) are excluded.

Because of the strong correlation, SM, especially on the timescale of about 5–7 days, could be monitored by satellite microwave measurements, as discussed by Jones and Vonder Haar (1997). Such observations would significantly increase knowledge about land surface hydrological processes and would lead to better climate predictions at both regional and continental scales (Rind 1982; Lakshmi et al. 1997).

In general, vegetation canopy architecture (shape, orientation, density, etc.) and land surface moisture and roughness affect the microwave radiative transfer within the vegetation layer (e.g., Ulaby et al. 1986; Jackson and Schmugge 1991; Le Vine and Karam 1996). As mean wind speed rises, the surface evaporation rate increases and dries the soil and vegetation. Also, winds can alternate the orientation and architecture of vegetation. A moderate, positive correlation between the pentad running means of the emissivities and wind speeds is found for all SSM/I channels (correlation coefficients are all $\sim$0.6). Similar correlation coefficients were found for all frequencies and polarizations, implying that steady winds change not only surface moisture but also other land surface properties.

c. Correlation of land surface microwave emissivities

The emissivities at different wavelengths should be correlated because many land surface properties, such as surface roughness, may be considered to be constant during the month, and the emittance over the range of

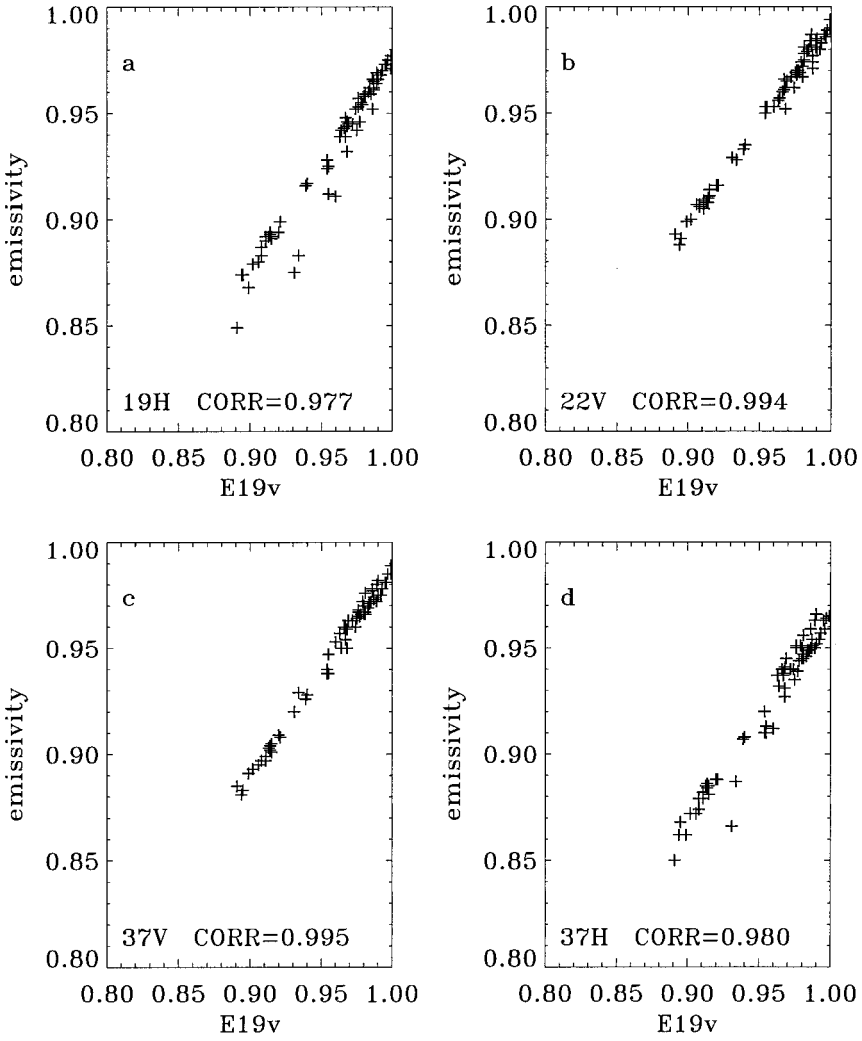

FIG. 8. The relationships of land surface microwave emissivities between 19v and (a)–(d) other SSM/I lower-frequency channels as labeled. CORR is correlation coefficient.

SSM/I frequencies increases with decreases in soil and vegetation moisture (Calvet et al. 1995a,b). The scatterplots of ε_i (Fig. 8) show the relationships between ε_{19v} and ε_i at other SSM/I low-frequency (<40 GHz) channels. The correlation coefficients are greater than 0.97 and tend to be higher for the same polarization than for those with different polarization. For example, the value between the 19v and 37v (0.995) channels is greater than that between the 19v and 19h (0.977) channels. For the 85-GHz channels, the relationships are basically the same as those shown in Fig. 8, although the correlation coefficients (>0.85) are slightly lower. Overall, no substantial relationship was found between ε_i and Δp (the absolute values of the correlation coefficients are <0.15; not shown here) because of the near-orthogonal nature of these quantities. The relationship between the various Δps (not shown here), on the other hand, is generally strong and positive, especially for Δp between 37 and 19 GHz. It is no surprise that closer wavelengths have stronger correlations.

The near-linear relationships found in Fig. 8 and the various Δps suggest that the SSM/I spectral emissivities are not statistically independent, at least over partially vegetated regions such as the ARM SGP site. The degrees of freedom should be significantly smaller than 7 so that the emissivities for all SSM/I channels can be estimated from two or three parameters. Thus, all of the independent variables desired from satellite remote sensing, such as ε_i, T_s, CWV, and LWP, may be estimated from a combination of microwave, visible, and infrared satellite measurements. For example, a microwave remote sensing method for surface and atmospheric properties over land could be accomplished by retrieving about five unknowns (about three emissivities, e.g., ε_{19v}, ε_{37h}, ε_{85h}, and LWP and CWV values) using all seven SSM/I channels. This idea actually

works well over oceanic environments. Over oceans, essentially only two parameters (near-surface wind speed and T_s) are used to estimate ε_i for all SSM/I channels. Then, all other major atmospheric and oceanic parameters that affect microwave radiation at SSM/I wavelengths can be retrieved simultaneously from combined microwave, visible, and infrared data (Lin et al. 1998b). Over land, no integrated methods are available to retrieve land surface and atmospheric parameters simultaneously. Prigent et al. (1997) proposed to modify a variational inversion method to estimate atmospheric properties over land. That approach still requires some prior information, however.

4. Concluding remarks

A unique dataset that combines surface observations and coincident SSM/I radiances was used to study intensively the remote sensing of microwave surface emissivity around the ARM site. Surface-based liquid water path and column water vapor data enabled the determination of surface emissivity on a relatively continuous basis during an entire month for both clear and cloudy conditions. The analyses revealed large temporal variations in surface microwave emissivities that arise primarily because of precipitation and surface and soil moisture changes. Despite the large emissivity variations, the strong correlations of emissivity among all of the SSM/I channels suggest that the number of independent variables for deducing emissivity is much less than seven. Thus, the emissivities at a few (e.g., three) SSM/I channels could be used to derive those for the other SSM/I frequencies and polarizations.

Approximately half of the variability in the estimated emissivities can be attributed to a substantial diurnal cycle that peaks in the early evening and reaches a minimum around sunrise. This almost daily variation appears primarily to be the result of dew formation and secondarily the result of cyclical changes in surface and vegetation moisture. The dew decouples the emissivity from the soil moisture variation. Dew effects are measurable with microwave radiances, but quantification of the condensation will require additional research. Elimination of data obtained during the early morning and during precipitation events reveals a strong correlation between soil moisture and surface emissivity and its differences for vertical and horizontal polarizations. Use of data measured at a particular satellite overpass time will reduce the emissivity variability substantially. The slow changes in the emissivities and polarization differences and the strong correlations of emissivity among all of the SSM/I channels should facilitate the determination of atmospheric parameters, such as cloud liquid water path and/or column water vapor, from combined satellite microwave, infrared, and visible measurements. Note, however, that only 1 month of data over one site has been examined. Much additional data must be examined in detail before any conclusive relationships can be developed. This study also confirms that soil moisture, especially the pentad mean values, can be monitored by combinations of microwave, visible, and infrared satellite measurements. Such a capability will significantly increase understanding of land surface hydrological processes. The effects of vegetation coverage and growth rate on microwave radiation require additional research. Measurements of dew, biomass, and vegetation water content would aid in that effort.

Acknowledgments. Support for this research was provided by Department of Energy Environmental Sciences Division Interagency Agreement #DE-AI02-97ER62341 as part of the Atmospheric Radiation Measurement Program and by the NASA Radiation Processes Program and the Earth Observing System (EOS)/ Interdisciplinary Program, NASA/Office of Mission to Planet Earth through the CERES Project. One of the authors (BL) thanks NASA for support under Contract NAS1-19656. Discussions with Dr. Bruce Wielicki are very helpful. The authors thank Dr. Tom Charlock for his CAGEX skin temperature data. Ground observations are obtained from the Atmospheric Radiation Measurement Program. The DMSP data were provided by the Distributed Active Archive Center at the NASA Marshall Space Flight Center in Huntsville, Alabama.

REFERENCES

Calvet, J., J. Wigneron, A. Chanzy, and D. Haboudane, 1995a: Retrieval of surface parameters from microwave radiometry over open canopies at high frequencies. *Remote Sens. Environ.,* **53,** 46–60.

——, ——, ——, S. Raju, and L. Laguerre, 1995b: Microwave dielectric properties of a silt-loam at high frequencies. *IEEE Trans. Geosci. Remote Sens.,* **33,** 634–642.

Charlock, T., and T. Alberta, 1996: The CERES/ARM/GEWEX Experiment (CAGEX) for the retrieval of radiative fluxes with satellite data. *Bull. Amer. Meteor. Soc.,* **77,** 2673–2683.

Choudhury, B., 1988: Microwave vegetation index: A new long-term global data set for biospheric studies. *Int. J. Remote Sens.,* **9,** 185–186.

Goodberlet, M. A., C. T. Swift, and J. C. Wilkerson, 1990: Ocean surface wind speed measurements of Special Sensor Microwave/ Imager (SSM/I). *IEEE Trans. Geosci. Remote Sens.,* **GE-28,** 832–828.

Hall, F., J. Townshend, and E. Engman, 1995: Status of remote sensing algorithms for estimation of land surface state parameters. *Remote Sens. Environ.,* **51,** 138–156.

Jackson, T., 1997: Soil moisture estimation using Special Satellite Microwave/Imager satellite data over a grassland region. *Water Resour. Res.,* **3,** 1475–1484.

——, and T. Schmugge, 1991: Vegetation effects on the microwave emission of soils. *Remote Sens. Environ.,* **36,** 203–212.

Jones, A., and T. Vonder Haar, 1997: Retrieval of microwave surface emittance over land using coincident microwave and infrared satellite measurements. *J. Geophys. Res.,* **102,** 13 609–13 626.

Justice, C. O., J. R. Townshend, and B. Choudhury, 1989: Comparison of AVHRR and SMMR data for monitoring vegetation phenology on a continental scale. *Int. J. Remote Sens.,* **10,** 1607–1632.

Kerr, Y., and E. Njoku, 1993: On the use of passive microwaves at

37 Ghz in remote sensing of vegetation. *Int. J. Remote Sens.,* **14,** 1931–1943.

Lakshmi, V., E. Wood, and B. Choudhury, 1997: Evaluation of Special Sensor Microwave/Imager data for regional soil moisture estimation over the Red River basin. *J. Appl. Meteor.,* **36,** 1309–1328.

Le Vine, D., and M. Karam, 1996: Dependence of attenuation in a vegetation canopy on frequency and plant water content. *IEEE Trans. Geosci. Remote Sens.,* **34,** 1090–1096.

Lin, B., and W. B. Rossow, 1997: Precipitation water path and rainfall rate estimates over oceans using Special Sensor Microwave Imager and International Satellite Cloud Climatology Project data. *J. Geophys. Res.,* **102,** 9359–9374.

——, B. Wielicki, P. Minnis, and W. B. Rossow, 1998a: Estimation of water cloud properties from satellite microwave, infrared, and visible measurements in oceanic environments. I: Microwave brightness temperature simulations. *J. Geophys. Res.,* **103,** 3873–3886.

——, P. Minnis, B. Wielicki, D. Doelling, R. Palikonda, D. Young, and T. Uttal, 1998b: Estimation of water cloud properties from satellite microwave, infrared, and visible measurements in oceanic environments. II: Results. *J. Geophys. Res.,* **103,** 3887–3905.

Mahfouf, J., E. Richard, and P. Mascart, 1987: The influence of soil and vegetation on mesoscale circulation. *J. Climate Appl. Meteor.,* **26,** 1483–1495.

McClatchey, R. A., R. W. Fenn, J. E. A. Selby, F. E. Voltz, and J. S. Garing, 1972: Optical properties of the atmosphere. Air Force Cambridge Research Laboratories Environmental Research Paper AFCRL-72-0497, No. 411, 108 pp.

Minnis, P., S. Mayor, W. Smith, and D. Young, 1997: Asymmetry in the diurnal variation of surface albedo. *IEEE Trans. Geosci. Remote Sens.,* **35,** 879–891.

——, W. L. Smith Jr., and D. F. Young, 1998: Surface emissivity derived from multispectral satellite data. *Proc. Eighth Annual ARM Science Team Meeting,* Tucson, AZ, U.S. Department of Energy, 489–494.

Prigent, C., W. Rossow, and E. Matthews, 1997: Microwave land surface emissivities estimated from SSM/I observations. *J. Geophys. Res.,* **102,** 21 867–21 890.

Raju, S., A. Chanzy, J. Wigneron, J. Calvet, Y. Kerr, and L. Laguerre, 1995: Soil moisture and temperature profile effects on microwave emission at low frequencies. *Remote Sens. Environ.,* **54,** 85–97.

Rind, D., 1982: The influence of ground moisture conditions in North America on summer climate as modeled in the GISS GCM. *Mon. Wea. Rev.,* **110,** 1487–1494.

Salisbury, J. W., and D. M. D'Aria, 1992: Emissivity of terrestrial materials in the 8–14 μm atmospheric window. *Remote Sens. Environ.,* **42,** 83–106.

Stokes, G. M., and S. E. Schwartz, 1994: The Atmospheric Radiation Measurement (ARM) Program: Programmatic background and design of the Cloud and Radiation Test Bed. *Bull. Amer. Meteor. Soc.,* **75,** 1201–1221.

Tucker, C., 1989: Comparing SMMR and AVHRR data for drought monitoring. *Int. J. Remote Sens.,* **10,** 1663–1672.

——, 1992: Relating SMMR 37 GHz polarization difference to precipitation and atmospheric carbon dioxide concentration: A reappraisal. *Int. J. Remote Sens.,* **13,** 177–191.

Ulaby, F., R. Moore, and A. Fung, 1986: *Microwave Remote Sensing.* Vol. 3. Addison–Wesley, 1097 pp.

Wigneron, J.-P., J.-C. Calvet, and Y. Kerr, 1996: Monitoring water interception by crop fields from passive microwave observations, *Agric. For. Meteor.,* **80,** 177–193.